Jpn. J. Appl. Phys. Vol. 36 (1997) pp. 7796–7800
Part 1, No. 12B, December 1997

Coulomb-Blockade Dominated Transport in Patterned Gold-Cluster Structures

Martin N. WYBOURNE[1*], Laura CLARKE[1], Mingdi YAN[2], Sui X. CAI[2], Leif O. BROWN[2], James HUTCHISON[2] and John F.W. KEANA[2]

[1]*Department of Physics, University of Oregon, Eugene, OR 97403, USA*
[2]*Department of Chemistry, University of Oregon, Eugene, OR 97403, USA*

(Received July 7, 1997; accepted for publication September 1, 1997)

In this paper we present the fabrication and near-room temperature electrical transport properties of structures made from the gold-cluster material $Au_{55}[P(C_6H_5)_3]_{12}Cl_6$. We discuss the use of electron-beam lithography to define the structures laterally and compare the direct current-voltage characteristics of non-patterned and patterned structures. In both cases non-linear behavior is observed with features that are consistent with Coulomb blockade dominated transport in disordered arrays of clusters. Radio frequency induced plateaus in the current-voltage characteristics demonstrate coherent tunneling. Finally, we show that other ligand stabilized gold-cluster materials can be used to form ordered gold-cluster arrays.

KEYWORDS: Coulomb-blockade, ligand stabilized metal cluster, disordered arrays, coherent electron tunneling, electron-beam lithography

1. Introduction

Devices working on the principle of Coulomb-blockade have been proposed as a way to overcome the predicted scaling limits associated with traditional semiconductor technology.[1,2] While Coulomb-blockade has been extensively studied at low-temperatures,[3,4] it has only recently been observed at room temperature in polycrystalline-silicon[5,6] and metal structures.[7] Coulomb-blockade is associated with the charge transport between metal or semiconductor islands coupled together by tunnel barriers. Two criteria are required for Coulomb-blockade. First, the Coulomb charging energy, E_c, of an island must be much larger than the ambient thermal energy, kT. Second, to avoid quantum fluctuations the tunnel barrier between islands must have a tunnel resistance greater than the quantum resistance h/e^2. Since the charging energy is given by $E_c = e^2/2C$, the first criterion can be satisfied by fabricating a system that has a small capacitance C. The second criterion is often met by isolating the islands by a dielectric. Various fabrication strategies for three- and two-dimensional arrays of small metal clusters have been reported.[8–11] In this paper we discuss the fabrication and transport properties of ligand stabilized gold-cluster structures. We report structures made from two classes of organometallic materials that have the same gold core (Au_{55}), but have different ligand shells. The majority of our discussion will concern the material dodeca(triphenylphosphine)hexa(chloro)pentaconta gold, $Au_{55}[P(C_6H_5)_3]_{12}Cl_6$. We present two different sample fabrication procedures; one using electron-beam irradiation to produce patterned devices,[12] the other non-patterned. In neither case was a post-fabrication anneal used to remove organic material. We show that the near-room temperature transport properties of both sample realizations have features consistent with the charging of individual Au_{55} cores.[13] The second class of materials we discuss have the Au_{55} metal core stabilized with either alkyl or aryl thiolate ligand shells. When drop cast onto a substrate these materials are found to self-assemble into close-packed arrays.[14] The important aspect of the Au_{55} material is the small size of the gold core which has an estimated radius, r, of 0.7 nm.[8] The core radius suggests that an isolated Au_{55} will have an extremely low geometrical capacitance, $C = 4\pi\varepsilon\varepsilon_0 r$, where ε is the dielectric constant of the surrounding medium. When ε is below ~ 4, the Coulomb charging energy exceeds the room temperature thermal energy by an order of magnitude. Under these conditions a Coulomb gap is developed at the Fermi level and energy E_c is required to place an extra electron onto the core. This energy must be provided by an external potential. Consequently, structures containing many cores isolated from each other by tunnel barriers are anticipated to have non-linear current-voltage (I–V) characteristics similar to those reported for tunnel junction arrays and single electron transistors operating at low temperature.[1,15,16] However, the highest temperature at which this non-linear behavior will be observed in an array is difficult to estimate *a priori* since additional capacitance due to the presence of other cores and a nearby ground plane will reduce the charging energy. The dynamic properties of arrays of metal islands will also be influenced by the presence of a Coulomb gap. For example, it has been predicted and demonstrated in other systems that tunneling events can be phase locked by an external radio frequency (RF) field whose frequency is related to the tunneling rate.[17]

2. Experiment

The gold cluster $Au_{55}[P(C_6H_5)_3]_{12}Cl_6$ was synthesized following the procedure of Schmid.[18] Various purification procedures were used to remove monomer material. Solutions of the gold cluster were made by dissolving between 21 and 22 mg of the solid in 0.25 mL of CH_2Cl_2 and 0.25 mL of CH_2ClCH_2Cl. For the preparation of the electron-beam-patterned samples, a solution was spin coated onto Si_3N_4 coated Si wafers at 1500 rpm for 25 seconds. The film was patterned by exposure to a 40 kV

*Present address: Department of Physics and Astronomy, Dartmouth College, 6127 Wilder Laboratory, Hanover, NH 03755, USA.

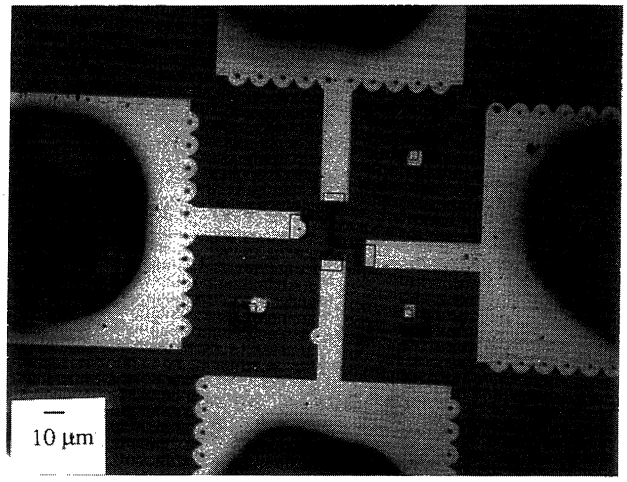

Fig. 1. An optical micrograph of the patterned gold cluster structure. The large bright regions are gold contacts. The patterned cluster material appears as the dark structure between contacts.

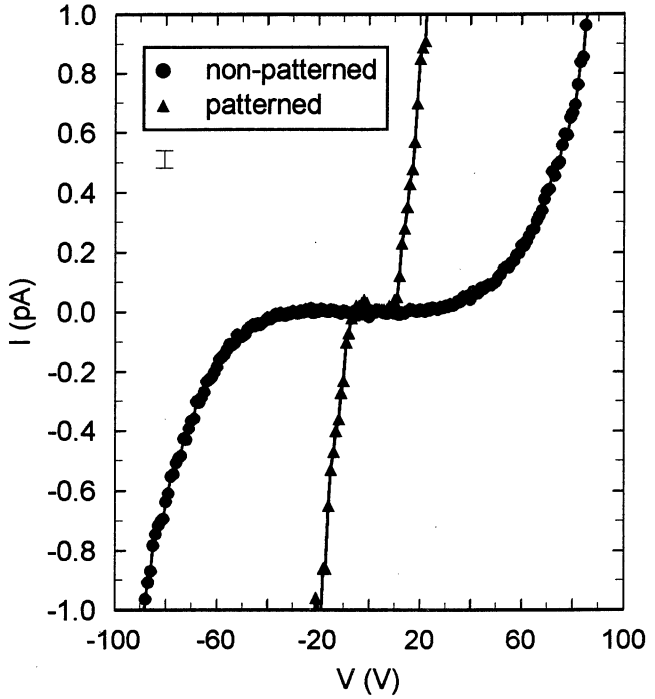

Fig. 2. The I–V characteristics for both patterned and non-patterned samples. The data for the patterned and non-patterned samples were taken at 195 and 295 K, respectively. These were the highest temperatures at which the current in the blockade regime was below the detectable limit. The error bar indicates the current error of each point.

electron-beam at a line dosage of 100 nC/cm. The areas of the film not exposed to the electron-beam were removed by a CH_2Cl_2 rinse. This procedure produced well-defined structures, as shown in Fig. 1, which appeared to be smooth and continuous under inspection by scanning electron microscopy. Attempts were made to pattern the material using 254 nm ultraviolet lithography, but it was found to be insensitive to this wavelength. The defined structures had dimensions as small as 0.1 μm and inspection by atomic force microscopy measured the film thickness to be 50 nm. The patterned organometallic samples were spin coated with poly(methyl methacrylate) which was electron-beam exposed and developed to define contact regions. Contacts were fabricated using thermal evaporation of 100 nm of gold and conventional liftoff procedures. The non-patterned samples were prepared by drop casting the solution onto a set of interdigitated gold electrodes on glass. The electrode separation was 15 μm.

Electrical transport measurements were made in an evacuated, shielded chamber, submerged in an oil bath. The oil bath temperature was controlled from 195 to 350 K. The samples were mounted on a clean Teflon stage and were connected to a constant direct-current (DC) voltage source and electrometer with triaxial lines. After thermal equilibration, the I–V characteristics showed little temperature drift over a typical four-hour sweep. The background leakage current of the apparatus set the minimum resolved conductance to be about $10^{-15}\,\Omega^{-1}$, with a current measurement resolution of 10 fA. Constant amplitude RF signals with frequencies, f, from 0.1 to 5 MHz, were applied to the samples via a dipole antenna at 195 K. Coupling between the RF signal and the sample was not optimized.

3. Results and Discussion

Both patterned and non-patterned samples displayed highly non-linear I–V behavior, as shown in Fig. 2, where the characteristics have been corrected to account for the leakage current of the apparatus. The electrical transport of the electron-beam-patterned sample at 195 K had current suppression up to a threshold voltage of magnitude 6.7 ± 0.6 V, above which the current increased abruptly. The magnitude of the threshold voltage did not change with time. The I–V characteristics of the non-patterned sample had a region of current suppression at 295 K, as shown in Fig. 2. Unlike the data from the patterned sample, the threshold voltage magnitude became smaller as a function of the time the bias was applied. The RF signal introduced plateaus in the I–V characteristics of both types of sample, as illustrated for the patterned sample in Fig. 3. While the RF introduced steps in the characteristics of the non-patterned samples, the step structure was not reproducible. This is likely related to a lower stability of the cluster configuration within non-patterned samples due to the absence of cross-linking between ligand shells. The issue of stability and ligand shell cross-linking is still under investigation so we restrict our discussion to the reproducible transport behavior found in the patterned samples. The current at which the plateaus occurred was found to be proportional to the applied signal frequency. Several distinct constants of proportionality were found with the highest being $1.59 \pm 0.04 \times 10^{-19}$ C, as shown in Fig. 4. The presence of RF induced steps indicates that transport in these systems is influenced by coherent single electron tunneling[17] which supports the notion that the non-linear I–V behavior is a result of Coulomb-blockade rather than some other mechanism.

Transport in ordered arrays of tunnel junctions and metal islands that have tunneling resistances larger than h/e^2 and a charging energy significantly above kT has

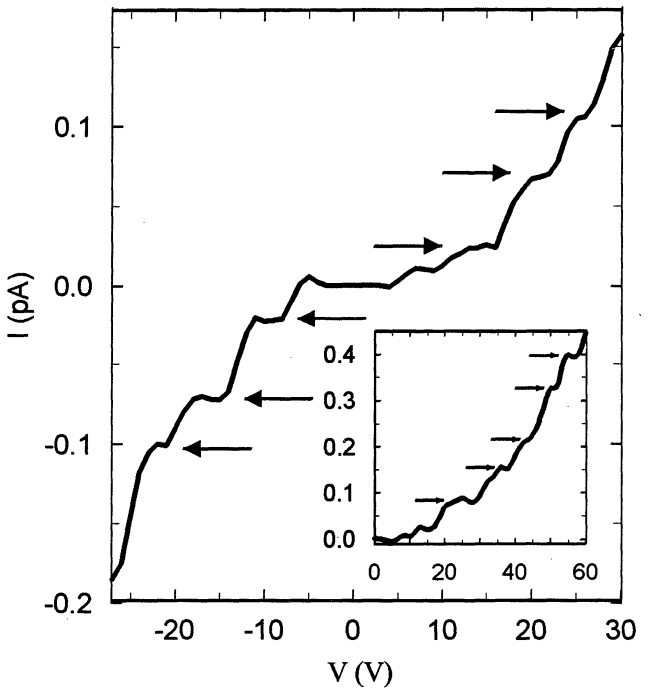

Fig. 3. The plateau structure for an applied RF signal of 0.626 MHz. The inset shows the plateau structure at 2.54 MHz. Both sets of data were obtained with a patterned sample at 195 K. Arrows indicate the plateaus.

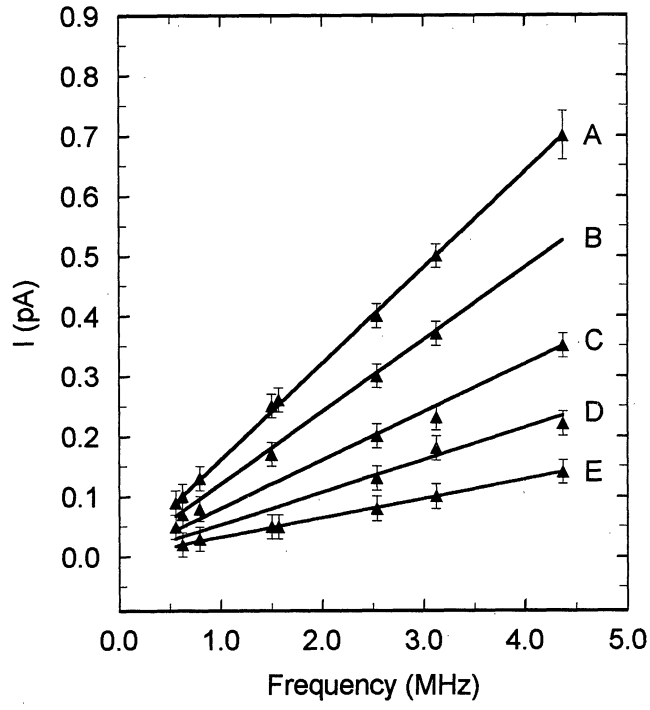

Fig. 4. The current at which plateaus occur as a function of applied frequency at 195 K. The solid lines have slopes, (A) e, (B) $3e/4$, (C) $e/2$ (D) $e/3$, and (E) $e/5$, where $e = 1.6 \times 10^{-19}$ C.

been modeled by several groups.[19–21] In all cases it is predicted that Coulomb charging introduces a threshold voltage below which current through the array is suppressed. As the applied voltage is increased well beyond threshold, the current-voltage characteristic approaches a linear asymptote with a slope related to the tunnel resistance. Under the same tunnel barrier and temperature constraints, Middleton and Wingreen have discussed one- and two-dimensional arrays of maximally disordered normal metal islands where disorder is introduced as random offset charges on each dot.[22] They predict current suppression below a threshold voltage, which scales with the number of junctions N along the current direction. Above threshold the current is predicted to scale as $I \sim (V/V_T - 1)^\gamma$. Analytically, γ is 1 for one-dimensional arrays and 5/3 for infinite two-dimensional arrays. Numerical simulations predict $\gamma = 2.0 \pm 0.2$ for finite two-dimensional arrays.[22] Since no attempt was made to order the gold core arrangement of either the patterned or non-patterned samples, it is expected that a disordered model should describe the data more closely. In all cases this expectation was confirmed by the behavior of the high current data which did not approach a linear asymptote predicted for ordered systems. Instead, the high current data scaled as predicted for disordered systems. For the electron-beam patterned sample $\gamma = 1.6 \pm 0.2$, and for the non-patterned samples $\gamma = 2.1 \pm 0.3$. Therefore, the non-patterned sample falls in the two-dimensional regime while the patterned sample appears to be between the one- and two-dimensional regimes. For all sets of data, the threshold voltages obtain from the scaling were consistent with the values estimated directly from the I–V data.

The RF induced plateau structure is similar to that reported in one-dimensional systems[23,24] and has been attributed to phase locking between single electron tunneling events and the RF.[17] Phase locking is possible in two-dimensional arrays, but inhomogeneities in the array are anticipated to smear the plateau structure. In the case of a very inhomogeneous two-dimensional array close to the percolation limit, a one-dimensional description should apply.[17] When the nth harmonic of the applied frequency corresponds to the mth harmonic of the frequency of tunneling in the system, mI/e, the current becomes locked to a value $I = (n/m)ef$. Therefore, the linear relationships shown in Fig. 4 agree with the hypothesis of correlated tunneling in the samples. From a best fit to the observed current positions of the steps we find the rational fractions 1/5, 1/3, 1/2, 3/4, and 1.

Over the temperature range 195 to 350 K the patterned samples had stable I–V characteristics, which above about 250 K developed activated conductance in the current suppression region. For various samples, the activation energies E_A were in the range 30 to 70 meV. Previously, the charging energy in an infinite two-dimensional array has been estimated from the measured activation energy by calculating the capacitance of a single island in the array and arguing that the Coulomb gap energy is twice the activation energy.[25] In the array the effective capacitance is twice that of an isolated island, thus $E_c \approx 4E_A$. The present samples are between the one- and two-dimensional regimes. Considering the core and ligand shell dimensions, each island in a one-dimensional array will have an effective capacitance of about 1.5 times that of an isolated island, thus $E_c \approx 3E_A$. Assuming current suppression requires $E_c \geq 10kT$, the sample with the largest activation energy should de-

velop a Coulomb gap below about 240 K or 300 K for the one- and two-dimensional cases, respectively. These values are close to the measured temperature at which blockade behavior is observed in the patterned samples. From these temperatures we find the effective capacitance of a metal core in the patterned array is in the range $3 \times 10^{-19} < C < 8 \times 10^{-19}$ F. These values are close, but larger than the classical geometric capacitance of an isolated Au_{55} cluster $C = 4\pi\varepsilon\varepsilon_0 r \approx 2 \times 10^{-19}$ F, where the dielectric constant of the surrounding ligand shell ε is expected to be approximately 3. The agreement between the two estimates of capacitance supports the idea that current suppression in the metal cluster arrays is due to charging of individual Au_{55} clusters.

Having established the capacitance of each core some constraints on the number of Au_{55} cores that make up the patterned array can be obtained from the measured threshold voltage and RF data. From the predicted threshold voltage in a disordered array, $V_T = \alpha Ne/C$,[22] where α is a parameter between 0 and 0.5 that depends on the ratio of the capacitance between cores to the capacitance to a ground plane. We find αN to be approximately 10. Unfortunately, it is not possible to determine N because we do not have enough structural information about the sample to estimate α reliably. Given the constraint that steps in the I–V characteristics are only found when $f < 0.1/(R_T C)$,[17] the fact that steps are seen up to $f = 5$ MHz gives the upper limit $R_T < 1 \times 10^{11}\,\Omega$. The differential resistance obtained from the I–V characteristic well above threshold is anticipated to be $R_{\text{diff}} \sim (N/M)R_T$, where M is the number of parallel channels in the array. This estimate yields $N/M \geq 30$. From the delineated sample dimensions and the size of an individual cluster, a close packed array would have $N/M \sim 5$. The large difference between the expected and experimentally derived values of N/M suggests that the full width of the sample is not involved in transport. One explanation for the discrepancy in N/M is that many of the gold cores coalesce during sample fabrication so that individual clusters between larger regions of gold dominate the transport.

A major difference between the electron-beam-patterned and the non-patterned samples is the long-term stability of the transport characteristics. Another difference is that blockade behavior in the non-patterned samples persists up to at least room temperature. We believe the transport in both cases is dominated by charging of single Au_{55} cores and that the enhanced stability of the patterned samples comes from a more rigid structure created by electron-beam-irradiation. Details of the electron-beam interaction with this organometallic material have yet to be determined. Particularly important will be an understanding of the cross-linking mechanism and the possibility that the electron-beam exposure may cause the gold core coalescence that appears to occur. However, it is clear that electron-beam exposure produces some form of cross-linking which effectively locks the metal cores in place creating a stable arrangement whose transport characteristics show Coulomb blockade effects close to room temperature.

One potential cause of instability in the $Au_{55}[P(C_6H_5)_3]_{12}Cl_6$ structures is the lability of the triphenylphosphine ligand shell.[26] Recently we have prepared thiol stabilized Au_{55} clusters with a gold to sulfur ratio of approximately 55 to 26. Assuming the gold core is Au_{55} this ratio corresponds to 25–26 thiolate ligands. UV visible spectroscopy studies show that these clusters exhibit dramatically improved thermal stability. Compared to the $Au_{55}[P(C_6H_5)_3]_{12}Cl_6$ clusters that decompose within about 1.5 h, the thiol stabilized clusters exhibit no decomposition after 24 h under the same conditions.[27] How this improved thermal stability will influence the electrical stability of a non-patterned, self-assembled sample is unknown at this time. Another advantage of the thiol ligand shell is that it promotes self-assemble into close-packed, monolayer arrays when drop cast onto a substrate, as shown by atomic force microscopy and TEM observations, as shown in Fig. 5.[14] Additionally, ligand exchange chemistry can be used to bond the cluster covalently to a rigid molecular scaffold to form ordered arrays and networks of metal clusters. Work is in progress toward the fabrication and electri-

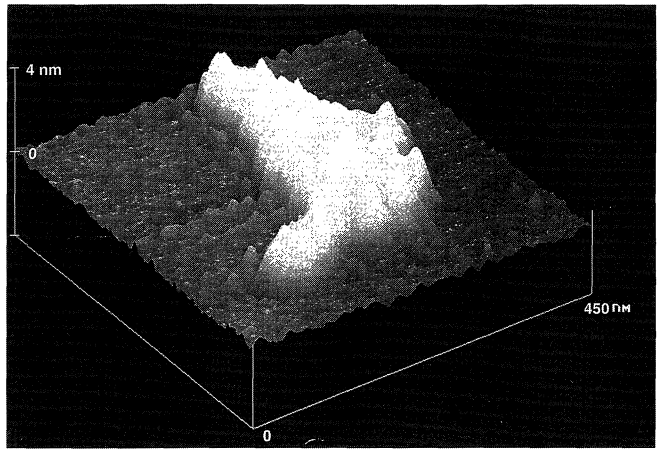

(a)

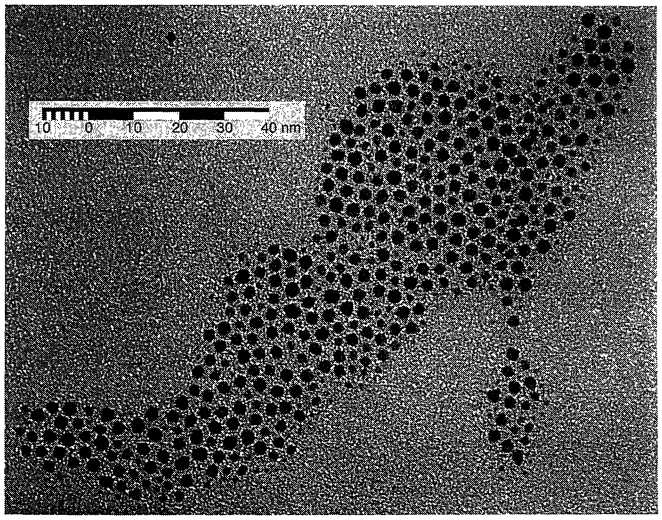

(b)

Fig. 5. (a) A monolayer island of octadecanethiol-stabilized Au_{55} nanoclusters assembled on mica as observed by tapping mode atomic force microscopy. (b) Transmission electron micrograph of ordered aggregates of biphenylmercaptan-stabilized gold nanoclusters.

cal characterization of these molecular scaffold organized networks.

Acknowledgements

This work was partially supported by the Office of Naval Research under contract numbers: N00014-93-0618 and N00014-93-1-1120. L. Clarke acknowledges supported from the Department of Education.

1) K. K. Likharev: *Granular Nanoelectronics*, eds. D. K. Ferry, J. R. Barker and C. Jacoboni (Plenum Press, New York, 1991) p. 371.
2) J. R. Tucker: J. Appl. Phys. **72** (1992) 4399.
3) J. Lambe and R. C. Jaklevic: Phys. Rev. Lett. **22** (1969) 1371.
4) See references, *Single Charge Tunneling Coulomb Blockade Phenomena in Nanostructures*, eds. H. Grabert and M. H. Devoret (Plenum Press, New York, 1992).
5) K. Yano, T. Ishii, T. Hashimoto, T. Kobayashi, F. Murai and K. Seki: Appl. Phys. Lett. **67** (1995) 828.
6) K. Yano, T. Ishii, T. Hashimoto, T. Kobayashi, F. Murai and K. Seki: IEEE Trans. Electron. Devices **41** (1994) 1628.
7) R. P. Andres, T. Bein, M. Dorogi, S. Feng, J. I. Henderson, C. P. Kubiak, W. Mahoney, R. G. Osifchin and R. Reifenberger: Science **272** (1996) 1323.
8) G. Schön and U. Simon: Colloid Polym. Sci. **273** (1995) 101.
9) A. P. Alivistos, K. P. Johnson, X. Peng, T. E. Wilson, C. J. Loweth, M. P. Bruchez Jr. and P. G. Schultz: Nature **382** (1996) 609.
10) R. P Andres, J. D. Bielefeld, J. I. Henderson, D. B. Janes, V. R. Kolagunta, C. P. Kubiak, W. J. Mahoney and R. G. Osifchin: Science **273** (1996) 1690.
11) D. L. Feldheim, K. C. Grabar, M. J. Natan and T. E. Mallouk: J. Am. Chem. Soc. **118** (1996) 7640.
12) M. Yan, S. X. Cai, J. C. Wu, C. A. Duchi, M. Kanskar, M. N. Wybourne and J. F. W. Keana: Poly. Mater. Sci. Eng. **70** (1994) 36.
13) L. Clarke, M. N. Wybourne, M. Yan, S. X. Cai and J. F. W. Keana: App. Phys. Lett. **71** (1997) 617.
14) L. Clarke, M. N. Wybourne, M. Yan, S. X. Cai, L. O. Brown, J. Hutchison and J. F. W. Keana: to be published in J. Vac. Sci. Technol. B (1997).
15) T. A. Fulton and G. J. Dolan: Phys. Rev. Lett. **59** (1987) 109.
16) A. J. Rimberg, T. R. Ho and J. Clarke: Phys. Rev. Lett. **74** (1995) 4714.
17) D. V. Averin and K. K. Likharev: *Mesoscopic Phenomena In Solids*, eds. B. Al'tshuler, P. Lee and R. A. Webb (Elsevier, Amsterdam, 1991).
18) G. Schmid: Inorgan. Synth. **27** (1990) 214.
19) N. S. Bakhvalov, G. S. Kazacha, K. K. Likharev and S. I. Serdyukova: Sov. Phys. JETP **68** (1989) 581.
20) N. S. Bakhvalov, G. S. Kazacha, K. K. Likharev and S. I. Serdyukov: Physica B **173** (1991) 319.
21) U. Geigenmüller and G. Schön: EuroPhys. Lett. **10** (1989) 765.
22) A. A. Middleton and N. S. Wingreen: Phys. Rev. Lett. **71** (1993) 3198.
23) L. J. Geerligs, V. F. Anderegg, P. A. M. Holweg, J. E. Mooij, H. Pothier, D. Esteve, C. Urbina and M. H. Devoret: Phys. Rev. Lett. **64** (1990) 2691.
24) P. Delsing, K. K. Likharev, L. S. Kuzmin and T. Claeson: Phys. Rev. Lett. **63** (1989) 1861.
25) T. S. Tighe, M. T. Tuominen, J. M. Hergenrother and M. Tinkam: Phys. Rev. Lett. **47** (1993) 1145.
26) G. Schmid: Chem. Rev. **92** (1992) 1709.
27) L. O. Brown and J. E. Hutchison: manuscript in preparation.